MLP-Assisted Agent Localization via Multipath Component Mapping

Seyeon Lee, Hongseok Jung, and Sunwoo Kim
Department of Electronic Engineering, Hanyang University, Seoul, South Korea
E-mail: {leah0900, hssjung, remero}@hanyang.ac.kr

***Abstract*—This paper proposes a multi-layer perceptron (MLP)-based localization framework for improving user equipment (UE) localization in mmWave simultaneous localization and mapping (SLAM) environments. The proposed framework learns the nonlinear relationship between multipath components and the UE position while incorporating previous predictions in a recursive manner, enabling accurate and temporally consistent positioning. By doing so, it overcomes the limitations of traditional closed-form algorithms, which produce unstable or inaccurate estimates in realistic indoor environments under noise and multipath propagation. The simulation results demonstrate that the MLP achieves an 83.76% reduction in the average RMSE computed over all time steps, compared with the traditional closed-form algorithm, and yields an estimated location of UE that closely matches the ground truth.**

***Index Terms*—Radio SLAM, reflection point, MLP**

I. Introduction

The radio simultaneous localization and mapping (SLAM) has been recognized as a fundamental enabling technique for 6G mmWave communication systems. This technology allows user equipment (UE) to perceive the surrounding environment, construct a map, and simultaneously estimate its own position [1], [2]. Radio-SLAM is particularly important in mmWave applications that require reliable positioning without relying on GPS signals, such as indoor navigation, autonomous robotics, and unmanned aerial vehicle (UAV) operation. By reconstructing the surrounding environment's geometry, the system can better interpret multi-path signals, thereby enabling robust and accurate UE trajectory estimation even in challenging indoor environments, where severe reflections, blockages, and NLOS conditions are common [3], [4].

Recent studies have advanced SLAM techniques in multipath mmWave environments through line-of-sight (LOS) and single-bounce non-line-of-sight (NLOS) signal identification strategies and outlier mitigation. However, these method approaches rely primarily on LOS measurements during localization and employ closed-form estimators that minimize algebraic errors rather than geometric distance errors, making it difficult to achieve precise and optimal positioning performance [5]. In addition, techniques that exhaustively evaluate all possible measurement-path combinations for valid path selection suffer from prohibitively high computational complexity as the number of reflections increases [6]. These limitations hinder conventional SLAM frameworks from providing robust and scalable localization performance in dense mmWave propagation environments. Other prior studies have likewise shown that closed-form localization methods, which assume ideal signal conditions, yield unstable and inaccurate position estimates under realistic multi-path and NLOS conditions [7], [8].

This work was supported by Institute of information communications Technology Planning Evaluation(IITP) grant funded by the Korea government(MSIT) (No. RS-2024-00337857, Development of Hybrid Positioning Technology for Emergency Rescue based on 5G and Multi-GNSS)

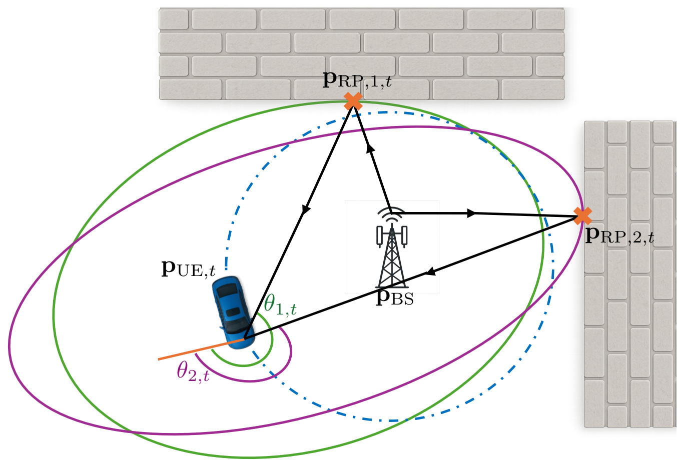

Fig. 1. Simulation environment and reflection-point mapping algorithm.

To address these challenges, this paper proposes a multi-layer perceptron (MLP)-based localization framework that improves localization accuracy in the mmWave SLAM scenario. The proposed approach exploits reflection points (RPs) derived from mapped NLOS paths to construct informative sensing features, enabling the MLP model to learn the nonlinear relationship between the multipath signal characteristics and the UE position. Furthermore, to support sequential localization, the framework adopts a recursive estimation process that leverages past position predictions as inputs for subsequent time steps, allowing the model to estimate the UE trajectory in a temporally consistent manner.

II. System Model

This paper considers a localization and mapping scenario consisting of a single base station (BS) and a single UE, as illustrated in Fig. 1. The BS is located at a fixed position denoted by $\mathbf{p}_{\mathrm{BS}} = [x_{\mathrm{BS}}, y_{\mathrm{BS}}]^\top$ and the 2D UE position at time t is defined as $\mathbf{p}_{\mathrm{UE},t} = [x_{\mathrm{UE},t}, y_{\mathrm{UE},t}]^\top$.

The UE receives a LOS signal and NLOS signals reflected from K walls. The corresponding measurements are modeled as

$$[\hat{d}_{k,t}, \hat{\theta}_{k,t}]^\top = [d_{k,t}, \theta_{k,t}]^\top + \mathbf{r}_{k,t} \tag{1}$$

where $\mathbf{r}_{0,t} \sim \mathcal{N}(0, \mathbf{R}_{\text{LOS}})$ for $k = 0$ and $\mathbf{r}_{k,t} \sim \mathcal{N}(0, \mathbf{R}_{\text{NLOS}})$ for $k = 1, \ldots, K$ denotes the measurement noise associated with the LOS and NLOS paths, respectively. $d_{k,t}$ and $\theta_{k,t}$ are the true propagation distance and unnoisy angle-of-arrival (AOA), respectively, and the LOS covariance matrix is given by $\mathbf{R}_{\text{LOS}} = \text{diag}(\sigma_d^2, \sigma_\theta^2)$. The parameters of the LOS and the k-th NLOS paths are given by

$$d_{k,t} = \begin{cases} \|\mathbf{p}_{\text{BS}} - \mathbf{p}_{\text{UE},t}\|, & k = 0 \\ \|\mathbf{p}_{\text{BS}} - \mathbf{p}_{\text{RP},k,t}\| + \|\mathbf{p}_{\text{RP},k,t} - \mathbf{p}_{\text{UE},t}\|, & \text{otherwise} \end{cases} \tag{2}$$

$$\theta_{k,t} = \begin{cases} \arctan \frac{\mathbf{p}_{\text{BS}} - \mathbf{p}_{\text{UE},t}}{\|\mathbf{p}_{\text{BS}} - \mathbf{p}_{\text{UE},t}\|}, & k = 0 \\ \arctan \frac{\mathbf{p}_{\text{RP},\mathbf{k},\mathbf{t}} - \mathbf{p}_{\text{UE},t}}{\|\mathbf{p}_{\text{RP},\mathbf{k},\mathbf{t}} - \mathbf{p}_{\text{UE},t}\|}, & \text{otherwise} \end{cases} \tag{3}$$

where $\mathbf{p}_{\text{RP},k,t} = [x_{\text{RP},k,t}, y_{\text{RP},k,t}]^\top$ is the position of RP.

Mapping is performed in all paths except the one corresponding to the smallest $\hat{d}$ value. Each path is assumed to involve a single bounce, where the signal propagates from the BS to the RP and then to the UE. The estimated RP's position is obtained by solving

$$\begin{cases} \|\hat{\mathbf{p}}_{\text{RP},k,t} - \mathbf{p}_{\text{BS}}\| + \|\hat{\mathbf{p}}_{\text{RP},k,t} - \mathbf{p}_{\text{UE},t}^{\text{LOS}}\| = \hat{d}, \\ (\hat{\mathbf{p}}_{\text{RP},k,t} - \mathbf{p}_{\text{UE},t}^{\text{LOS}})^\top \mathbf{u}_{k,t} = \|\hat{\mathbf{p}}_{\text{RP},k,t} - \mathbf{p}_{\text{UE},t}^{\text{LOS}}\|, \end{cases} \tag{4}$$

where $\mathbf{u}_{k,t} = [\cos(\hat{\theta}_{k,t}), \sin(\hat{\theta}_{k,t})]^\top$ denotes the unit direction vector, and $\mathbf{p}_{\text{UE},t}^{\text{LOS}}$ is the approximate UE position derived from LOS measurements via Jacobian linearization. The RP lies on an ellipse having the BS and the UE as its foci, and simultaneously on a straight line originating from the UE in the direction of the $\mathbf{u}_{k,t}$. The RP's position is determined as the intersection between the line and the ellipse, as illustrated in Fig. 1.

III. MLP - based Sequential localization model

The proposed framework employs an MLP architecture composed of an input layer, multiple hidden layers, and an output layer. This structure is selected to effectively capture the non-linear relationships induced by multipath propagation [9]. For each hidden layer l, the activation vector is computed as

$$\mathbf{h}^l = \mathbf{g}(\mathbf{W}^l \mathbf{h}^{l-1} + \mathbf{b}^l), \tag{5}$$

where $\mathbf{g}(\cdot)$ denotes the non-linear activation function, $\mathbf{W}^l \in \mathbb{R}^{N_l \times N_{l-1}}$ is the weight matrix connecting layer $l-1$ to l, and $\mathbf{b}^l \in \mathbb{R}^{N_l}$ is the bias vector. This paper employs two MLP models sharing this architecture: Model A for single-step localization and Model B for recursive sequential positioning. The input to Model A is constructed by aggregating $\hat{\mathbf{p}}_{\text{RP},k,t}$, $\hat{d}_{k,t}$, and $\hat{\theta}_{k,t}$ obtained from all K NLOS paths at time t:

$$\mathbf{x}_t = [\hat{\mathbf{p}}_{\text{RP},1,t}^\top, \hat{d}_{1,t}, \hat{\theta}_{1,t}, \cdots, \hat{\mathbf{p}}_{\text{RP},K,t}^\top, \hat{d}_{K,t}, \hat{\theta}_{K,t}]. \tag{6}$$

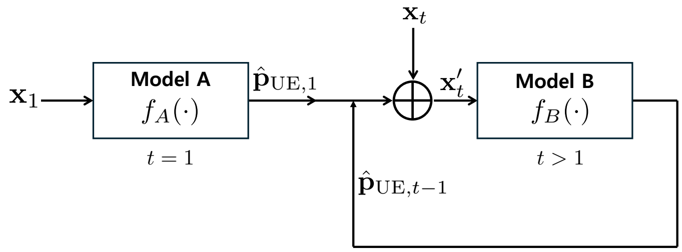

Fig. 2. Recursive MLP-based localization: Model A initializes the position at $t = 1$, and Model B recursively updates it using prior estimates.

For sequential localization, Model B augments $\mathbf{x}_t$ with the previously estimated UE position:

$$\mathbf{x}_t' = [\mathbf{x}_t, \hat{\mathbf{p}}_{\text{UE},t-1}^\top]. \tag{7}$$

For both models, these input vectors serve as the initial activation to the hidden layer, that is,

$$\mathbf{h}^0 = \begin{cases} \mathbf{x}_t, & \text{Model A} \\ \mathbf{x}_t', & \text{Model B} \end{cases} \tag{8}$$

Since no historical estimate is available at $t = 1$, the initial UE position is obtained using Model A: $\hat{\mathbf{p}}_{\text{UE},1} = f_A(\mathbf{x}_t)$, while for $t > 1$, Model B performs recursive localization according to $\hat{\mathbf{p}}_{\text{UE},t} = f_B(\mathbf{x}_t')$ where $f_A(\cdot)$ and $f_B(\cdot)$ are the trained MLP model. This recursive structure of the estimation process is illustrated in Fig.2, enables consistent trajectory tracking by incorporating past position estimates into each subsequent prediction.

IV. Simulation Results

An $60\,\text{m} \times 60\,\text{m}$ indoor environment is considered with a fixed BS that is located at $[0\,\text{m}, 0\,\text{m}]^\top$, and a UE moving along a circular trajectory around it.

A. Training MLP model

To generate the training dataset, the parameters of the simulation are configured as follows. The noise covariance matrix of measurements $\mathbf{R}_{\text{LOS}}$, and $\mathbf{R}_{\text{NLOS}}$ are set to $\text{diag}(0.25\,\text{m}^2, 10^{-4}\,rad^2)$, $\text{diag}(9\,\text{m}^2, 10^{-2}\,rad^2)$, respectively. The overall time duration for completing one circular trajectory is set to $T = 40$ time steps, and 100 unique scenarios are used as the training data. Both Model A and B adopt an MLP architecture composed of $L = 2$ connected hidden layers with 64 neurons each, and apply the rectified linear unit (ReLU) as the activation function $\mathbf{g}(\cdot)$ in each hidden layer. The models are trained using the Adam optimizer with a learning rate of 0.001, while the MSE is used as the loss function. Training is performed for up to 500 epochs with a batch size of 32.

To validate the effectiveness of the proposed framework, the performance is compared against a traditional closed-form algorithm, Levenberg-Marquardt (LM), using the same test dataset. The test dataset is constructed to be entirely disjoint from the training data and is generated by simulating 10 circular trajectories of the UE.

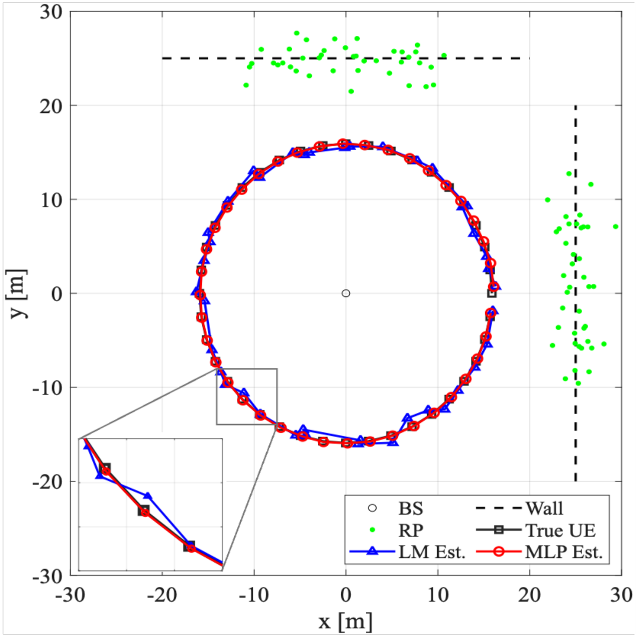

Fig. 3. Illustration of mapping and localization, showing the UE trajectories estimated by the LM and the proposed MLP framework.

B. Results and Discussion

As shown in Fig. 3, we compare with the traditional LM method and our proposed MLP-based localization framework. Although the LM algorithm generally traces the overall circular path, it exhibits noticeable local distortions, including radial deviations and shape irregularities, particularly in regions where the induced multi-path RP estimates are highly dispersed. In contrast, the trajectory produced by the MLP closely aligns with the true circular motion, forming a smooth and nearly distortion-free path despite the noisy and spatially scattered RP estimates. This significant improvement highlights the ability of the MLP to learn the nonlinear relationships between the geometry of the RP and the position of the UE, resulting in substantially robust localization. Overall, the visual comparison clearly demonstrates the enhanced robustness of the proposed learning-based approach in dense mmWave multi-path environments.

Table. I presents the localization RMSE for the proposed MLP framework and the LM algorithm across varying total-distance noise levels. At the lowest noise level, the RMSE of the LM algorithm is $0.30\,\mathrm{m}$, and the MLP achieves an RMSE of $0.08\,\mathrm{m}$. This performance gap widens as noise increases: the LM's RMSE reaches $1.00\,\mathrm{m}$, whereas the MLP maintains a significantly smaller error of $0.13\,\mathrm{m}$. On average, the framework reduces the localization error by approximately 83.76% relative to the LM. These results demonstrate that the proposed learning-based approach is markedly more robust to measurement noise than the closed-form LM estimator.

Table. II shows the localization performance of the LM algorithm and the proposed MLP framework under varying AOA noise levels. The LM algorithm is particularly vulnerable, with RMSE rising sharply from $0.55\,\mathrm{m}$ to $1.25\,\mathrm{m}$. By contrast, the framework maintains substantially lower RMSE, achieving $0.08\,\mathrm{m}$ at 1° and $0.31\,\mathrm{m}$ at 4°. The MLP framework achieves 76.76% reduction in localization average error compared with the LM algorithm, and the performance gap between the two methods increases as the noise level becomes larger. Moreover, the error growth rate under noise is significantly more moderate in the MLP case, demonstrating its robustness to angular measurement uncertainty.

TABLE I
RMSE COMPARISON OF MLP AND LM ACROSS DISTANCE NOISE LEVELS.

σ_d	$0.1\,\mathrm{m}$	$0.4\,\mathrm{m}$	$0.7\,\mathrm{m}$	$1.0\,\mathrm{m}$
LM	$0.30\,\mathrm{m}$	$0.50\,\mathrm{m}$	$0.75\,\mathrm{m}$	$1.00\,\mathrm{m}$
MLP	$0.08\,\mathrm{m}$	$0.10\,\mathrm{m}$	$0.11\,\mathrm{m}$	$0.13\,\mathrm{m}$

TABLE II
RMSE COMPARISON OF MLP AND LM ACROSS AOA NOISE LEVELS.

σ_θ	1°	2°	3°	4°
LM	$0.55\,\mathrm{m}$	$0.74\,\mathrm{m}$	$0.96\,\mathrm{m}$	$1.25\,\mathrm{m}$
MLP	$0.08\,\mathrm{m}$	$0.19\,\mathrm{m}$	$0.23\,\mathrm{m}$	$0.31\,\mathrm{m}$

V. CONCLUSION

This paper proposed an MLP-based localization framework that improve UE position estimation accuracy in noisy and multipath mmWave SLAM environments by learning the nonlinear relationship between LOS, NLOS sensing features and UE position. This framework also performs localization recursively by feeding the previously estimated position into the next prediction step, allowing it to preserve temporal continuity and accurately track the UE trajectory over time. Simulation results show substantial RMSE reduction and trajectory estimates that closely follow the ground truth, demonstrating that the MLP-based approach is more effective than the traditional closed-form algorithms. Future work may extend multi-agent operation and cooperative localization.

REFERENCES

[1] H. Que, J. Yang, T. Du, S. Xia, C.-K. Wen, and S. Jin, "Cooperative mapping, localization, and beam management via multi-modal slam in isac systems," *IEEE Trans. Commun.*, 2025.

[2] L. Wielandner, E. Leitinger, F. Meyer, and K. Witrisal, "Message passing-based 9-d cooperative localization and navigation with embedded particle flow," *IEEE Trans. Signal Inf. Process. Netw.*, vol. 9, pp. 95–109, 2023.

[3] J. Yang, C.-K. Wen, J. Xu, H. Que, H. Wei, and S. Jin, "Angle-based slam on 5g mmwave systems: Design, implementation, and measurement," *IEEE Internet Things J.*, vol. 10, no. 20, pp. 17 755–17 771, 2023.

[4] E. Leitinger, L. Wielandner, A. Venus, M. Liang, F. Meyer, and K. Witrisal, "Multipath-based slam with cooperation and map fusion in mimo systems," in *Proc. Asilomar Conf. Signals Syst. Comput*, 2024, pp. 1316–1322.

[5] Y. Ge, M. F. Keskin, H. Chen, O. Kaltiokallio, M. Li, M. Valkama, C. Masouros, and H. Wymeersch, "Pilot-based end-to-end radio positioning and mapping for isac: Beyond point-based landmarks," *arXiv*, 2025.

[6] O. Kaltiokallio, E. Rastorgueva-Foi, J. Talvitie, Y. Ge, H. Wymeersch, and M. Valkama, "Robust snapshot radio slam," *IEEE Trans. Veh. Technol.*, 2024.

[7] Y. Sun, K. Ho, and Q. Wan, "Solution and analysis of tdoa localization of a near or distant source in closed form," *IEEE Trans. Signal Process.*, vol. 67, no. 2, pp. 320–335, 2018.

[8] S. P. Ahmadi, A. Hansson, and S. K. Pakazad, "Distributed localization using levenberg-marquardt algorithm," *EURASIP J. Adv. Signal Process*, vol. 2021, no. 1, p. 74, 2021.

[9] J. Singh and R. Banerjee, "A study on single and multi-layer perceptron neural network," in *Proc. Int. Conf. on Computing Methodologies and Communication (ICCMC)*, 2019, pp. 35–40.